



Publication Year	2017
Acceptance in OA	2020-12-17T15:16:25Z
Title	ASPIICS/PROBA-3 formation flying solar coronagraph: Stray light analysis and optimization of the occulter
Authors	Romoli, M., Vivès, S., Mazzoli, A., LANDINI, FEDERICO, MASSONE, Giuseppe, Lamy, P., Venet, M.
Publisher's version (DOI)	10.1117/12.2309173
Handle	http://hdl.handle.net/20.500.12386/28947
Serie	PROCEEDINGS OF SPIE
Volume	10565

ASPIICS/PROBA-3 FORMATION FLYING SOLAR CORONAGRAPH: STRAY LIGHT ANALYSIS AND OPTIMIZATION OF THE OCCULTER

F. Landini^{*1}, A. Mazzoli², M. Venet³, S. Vives³, M. Romoli¹, P. Lamy³, G. Massone⁴

¹*Dipartimento di Fisica e Astronomia – Sez. Astronomia, Univ. di Firenze, Italy.*

FL: flandini@arcetri.astro.it, MR: romoli@arcetri.astro.it

²*Centre Spatial de Liège, Univ. de Liège, Belgium; amazzoli@ulg.ac.be*

³*Laboratoire d'Astrophysique de Marseille, France;*

MV: melanie.venet@oamp.fr, SV: Sebastien.Vives@oamp.fr, PL: philippe.lamy@oamp.fr

⁴*INAF – Osservatorio Astronomico di Torino, Italy; massone@oato.inaf.it*

** Contact author.*

I. INTRODUCTION

The “Association de Satellites Pour l’Imagerie et l’Interferometrie de la Couronne Solaire”, ASPIICS, selected by ESA for the PROBA-3 mission, heralds the next generation of coronagraph for solar research, exploiting formation flying to gain access to the inner corona under eclipse-like conditions for long periods of time. A detailed description of the ASPIICS instrument and of its scientific objectives can be found in [1].

ASPIICS is distributed on the two PROBA 3 spacecrafts (S/C) separated by 150 m. The coronagraph optical assembly is hosted by the “coronagraph S/C” protected from direct solar disk light by the occulting disk on the “occulter S/C”.

The most critical issue in the design of a solar coronagraph is the reduction of the stray light due to the diffraction and scattering of the solar disk light by the occulter, the aperture and the optics. In the present article, we deal with two of these issues:

- The analysis of the stray light inside the telescope.
- The optimization of the external occulter edge, in order to eliminate the Poisson spot behind the occulter and to lower the stray light level going through the entrance pupil of the telescope.

This work was performed in the framework of the ESA STARTIGER program which took place at the Laboratoire d’Astrophysique de Marseille (LAM) during a 6-month period from September 2009 to March 2010.

In general, it is a very complicated task to combine the above two stray light issues together in the simulation and design phase as it requires to consider the propagation inside the telescope of the light diffracted by the external occulter. Actually, the present literature only reports diffraction calculations performed for simple occulting systems (i.e., two disks and serrated disk). A more pragmatic approach, also driven by the tight schedule of the STARTIGER program, is to separate the two contributions, and perform two different stray light analyses. This paper is dedicated to the description of both analyses: in particular, the first part is dedicated to the evaluation of the stray light inside the telescope, assuming a simple disk as occulter, and a preliminary baffle design is presented; the second part describes the investigation on the geometry of the external occulter, with a detailed description of the laboratory setup that has been designed and implemented to compare together several types of occulting systems.

II. OPTICAL DESIGN

For our present purpose, we consider an occulter, 150 m away from the telescope optical assembly whose optical design follows the general principles of a classical externally occulted Lyot coronagraph [2].

The external occulter (EO) blocks the light from the solar disk while the coronal light passes through the entrance aperture (100 mm diameter). An unobstructed three-mirror anastigmat (TMA) is selected to limit the optical aberrations and the total length of the instrument while allowing a larger F-number of F/7. The primary mirror is placed about 800 mm behind the entrance pupil. The internal occulter (IO) is located at the conjugate plane of EO which is just after the focal plane of the TMA, and partly blocks the light diffracted by the EO edge.

The optical components that give a major contribution to the stray light level on the focal plane of the whole telescope are included in the optical path between the two conjugate planes of EO and IO. We presently limit our analysis to the IO plane, leaving to a future phase the complete analysis of stray light propagation to the focal plane of the coronagraph.

III. TELESCOPE STRAY LIGHT ANALYSIS

In order to properly simulate the stray light non-sequential propagation inside the telescope, a 3D model was built using the ASAP[®] ray tracing software. Besides the optical components, the structure of the telescope is included to make the calculation as realistic as possible.

A. Preliminary baffles design

The internal occulter can directly see the entrance pupil only through reflections on the TMA mirrors. To eliminate this stray light contribution, three baffles have been placed inside the TMA. They can be seen in Fig. 1b. In order to limit the stray light produced by sources outside the field-of-view, a tube is used as an entrance baffle to the TMA (see Fig. 1a) and vanes are added inside to prevent stray light reflected by the tube inner surface to enter the TMA.

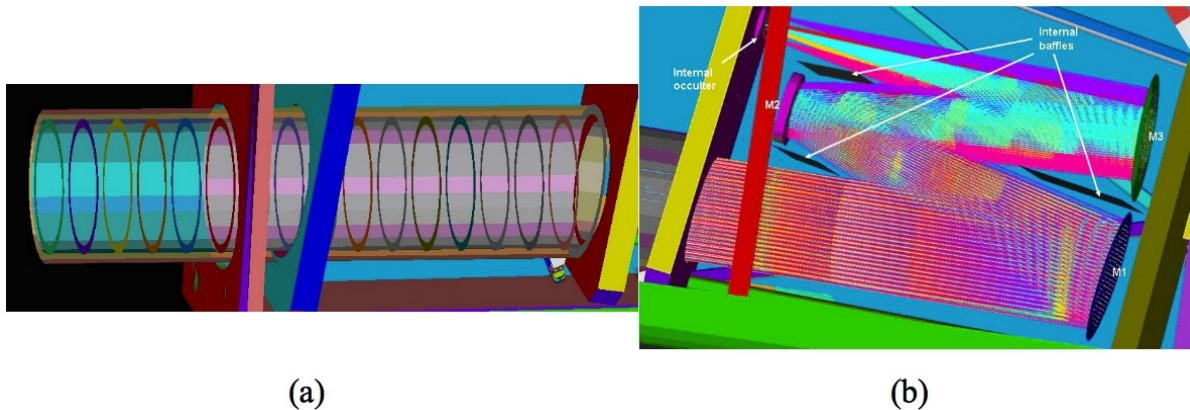


Fig. 1. (a) Vanes inside the entrance tube. (b) Baffles inside the TMA

B. Mirrors micro-roughness

Different micro-roughnesses have been applied in the ASAP[®] model to the 3 mirrors of the TMA in order to check their impact in term of stray light level at the IO plane. The roughnesses were introduced as bidirectional reflectance distribution function models using the Harvey-Shack mathematical model. Five roughnesses have been considered (0.2, 0.5, 1, 2 and 5 nm) and the results are presented in Table 1, which shows also the TIS (total integrated scatter) corresponding to each roughness. The most important outcome is that all mirrors give a similar stray light level for the same roughness which indicates that no mirror is dominant in term of scattered stray light. From the table and the specification on the maximum acceptable stray light level at the IO plane, the maximum micro-roughnesses requirement of the mirrors can be set.

Table 1. Stray light rejection factors at the IO plane for different mirror roughnesses and corresponding TIS

Roughness (nm)	TIS	M1	M2	M3
0.2	$2.2 \cdot 10^{-5}$	$6 \cdot 10^{-6}$	$7.2 \cdot 10^{-6}$	$7.4 \cdot 10^{-6}$
0.5	$1.4 \cdot 10^{-4}$	$1 \cdot 10^{-4}$	$8.3 \cdot 10^{-5}$	$1.1 \cdot 10^{-4}$
1.0	$5.6 \cdot 10^{-4}$	$4.2 \cdot 10^{-4}$	$3.3 \cdot 10^{-4}$	$4.4 \cdot 10^{-4}$
2.0	$2.2 \cdot 10^{-3}$	$1.7 \cdot 10^{-3}$	$1.3 \cdot 10^{-3}$	$1.8 \cdot 10^{-3}$
5.0	$1.4 \cdot 10^{-2}$	$1.2 \cdot 10^{-2}$	$7.5 \cdot 10^{-3}$	$1.3 \cdot 10^{-2}$

C. Diffraction from the external occulter

In order to estimate the stray light contribution given by the solar disk light diffracted by the EO, we followed a two-steps procedure. First, we calculated the diffraction pattern at the entrance pupil of the coronagraph) and then, we propagated the obtained pattern through the optical components of the coronagraph up to the plane of IO using ASAP[®].

The diffraction pattern was calculated analytically because it would have required too large a computation time with ASAP[®] to reach the desired accuracy. The Fresnel-Kirchhoff based analytical diffraction calculation can give the pattern corresponding to the whole disk but an annular source with the size of the disk cannot be

defined in ASAP[®]. Therefore it was decided to approximate the EO as a series of small linear occulters distributed along the edge circumference and use point sources distributed along the EO edge in ASAP[®].

For the analytical calculation, an extended source with the size of the Sun has been considered. The diffraction pattern behind a linear occulter is a relatively easy to calculate, even considering an extended source. Using the well known Huygens-Fresnel theory [3], the normalized diffracted light intensity pattern behind a knife-edge for a point source at infinity is given by:

$$I(x; \lambda) = \left| \frac{1}{2} \left[(C(\alpha) - S(\alpha)) + i(1 + C(\alpha) + S(\alpha)) \right] \right|^2 \quad (1)$$

where λ is the wavelength, x is the coordinate in the image plane along the direction perpendicular to the occulter edge, $\alpha = x\sqrt{2/(\lambda L)}$, with L the distance between the occulter and the image plane, i is the imaginary unit and $C(\alpha)$ and $S(\alpha)$ are the Fresnel integrals.

By integrating equation (1) over the solar disk, after some brief analytical calculation, we obtained:

$$I_s(x; \lambda) = \frac{1}{\pi R_\odot^2} \int_{-R_\odot+x}^{R_\odot+x} \left[(1 + C(\alpha_s))^2 + (1 + S(\alpha_s))^2 \right] B(x_s) dx_s \quad (2)$$

where x_s is the coordinate along the solar disk radius, $\alpha_s = \sqrt{2/(\lambda L)}(x - x_s)$ and $B(x_s) = \sqrt{R_\odot^2 - (x - x_s)^2}$.

The diffraction pattern at the entrance aperture plane, due to a linear portion of the EO, calculated by means of (1) and (2) along a direction perpendicular to the portion itself, has a behaviour analog to that shown in Fig. 5 (black solid line). The origin of the x -axis corresponds to the point where the line defined by the center of the Sun and the center of the occulter edge intersects the image plane. In order to propagate with ASAP[®] this stray light through the TMA, the profile of the diffraction pattern along one pupil diameter is not sufficient. The whole pattern in the entrance aperture is necessary. As a first approximation and due to the large dimension of the occulter (1.5 m in diameter) with respect to the pupil diameter (100 mm), we obtained the 2D pattern on the pupil by patching several times the line profile we obtained from (1) and (2). A view of the pattern in the pupil as generated by one of the portions of EO is shown in Fig. 2: it corresponds to a source placed on the edge in the negative part of the Y axis. Depending on the position of the source on the occulter edge, this kind of distribution in the pupil is rotated (in order to take into account the position of the considered EO edge portion with respect to the pupil position), then normalized to the total number of portions.

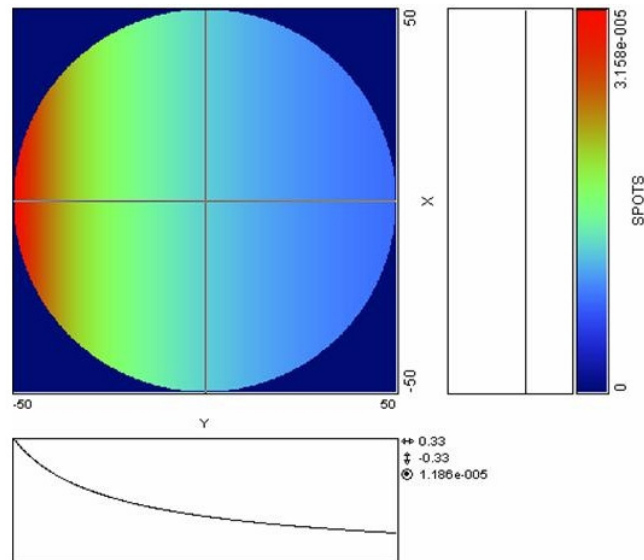


Fig. 2. Pattern of energy distribution due to the diffraction by one linear portion of the EO at the TMA entrance pupil

The next step is the propagation of each pattern through the optical and structural models of the TMA built with ASAP[®]. To do this, several points source were placed on the edge of EO assuming an intensity distribution of each beam given by the diffraction pattern calculated by means of (1) and (2). The flux level we used per each source is equal to the normalized flux given by the diffraction pattern calculation, divided by the number of

considered sources. Fig. 3a shows the geometrical computation for several points source distributed on the occulter edge.

To see more clearly the structure inside the ring in the IO plane, it is necessary to enlarge a small part of it. To do this, several sources are placed close to each other on a small part of the occulter edge. The visualization window in the IO plane is also chosen centered on the image, with enough pixels to see the details of the diffraction pattern. An example of the radial stray light behaviour is presented in Fig. 3b.

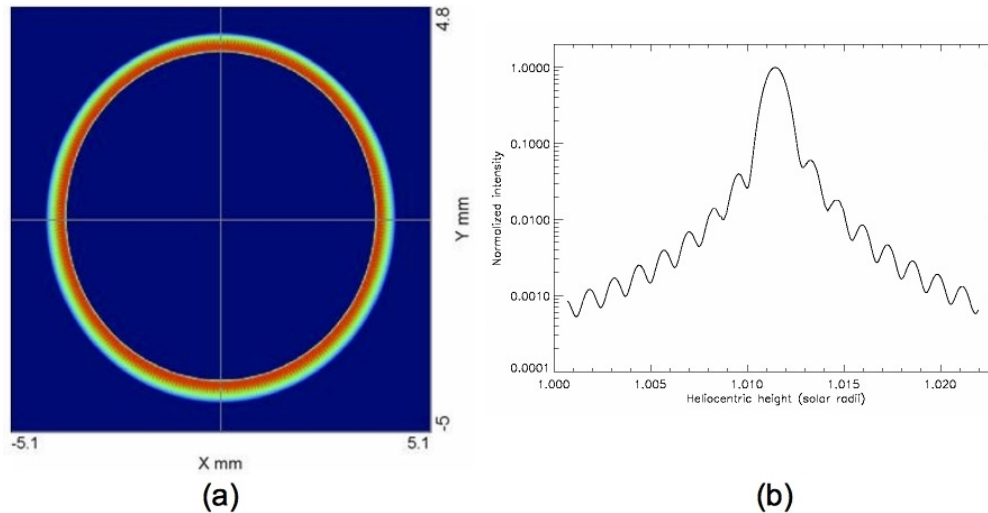


Fig. 3. (a) Stray light pattern in the IO plane. (b) Zoom on a small part of the pattern: associated radial profile

IV. EXTERNAL OCCULTER OPTIMIZATION

In classical externally occulted coronagraphs, special attention must be paid to the optimization of the occulting disk. Unlike past coronagraphs, the dimensions of ASPIICS (the EO has a diameter of ~ 1.5 m) preclude working with a full scale occulter. This section below presents an alternative by considering short linear portions approximating its large outer edge, in line with the above simulation.

In the solar physics community, there have been long debates on the most efficient system in stray light reduction for coronagraphic occulting systems. The following systems have been classical considered: toothed disk, triple disk, multithreaded and polished truncated cones. The only system theoretically fully analyzed is the toothed disk [4], while the triple disk and the multi-thread solution are only qualitatively explained and experimentally tested. In particular, Koutchmy [5] and Bout [6] reported experimental and theoretical (where possible) comparisons among different systems.

A. ASPIICS requirements

ASPIICS inner field-of-view (FOV) is $1.015 R_{\odot}$ and this, a priori, tends to preclude using a toothed disk. In fact, even by using a tiny peak-to-valley distance of 5 mm (that would mean a number of teeth of about 5000 and a peak-to-peak distance of $50 \mu\text{m}$), the inner limit of the FOV would be increased to $1.02 R_{\odot}$. The pointing stability is another requirement that has to be considered: the spacecraft must keep the alignment within strict tolerances. This constraint suggests avoiding long occulting systems, such as the multiple disks, but also a cone would have to be short, i.e. $\sim 10\div 15$ cm at most. For conic occulters, the material, the machining and the surface finish can all affect the performances and laboratory tests are needed to assess these unexplored aspects.

Since polished or electro-eroded cones (or barrels) are more easily machined and less expensive than multi-threaded ones while offering comparable performances [6], we decided to concentrate first on the former ones. Due to the aforementioned ASPIICS constraints, those occulters must be short so that cones and barrels will differ by negligible amounts. However, compact barrels with different design principles can be investigated (see subsection D below).

B. Laboratory setup

A test set-up has been designed and realized at LAM, inside a class 100 clean room using the solar simulator implemented for the tests of the LASCO-C2 coronagraph [6]. Since it is practically impossible to realize a full-scale model of ASPIICS, we designed a set-up able to measure the stray light behind a section of the whole occulter. The section of such a large occulter (1.5 m diameter) can be well approximated by a small straight

edge piece. We therefore measured the diffraction pattern behind a linear occulter and not behind a disk, thus it is not possible to directly extrapolate our present results to the actual coronagraph, but it is possible to perform a relative analysis, by comparing stray light reduction performances of linear occulters with respect to the reference knife-edge (this case is easily computable even for an extended source, see (1) and (2) and black solid line in Fig. 5).

A complete overview of the set-up is shown in Fig. 4a: the source is coupled to a collimator in order to simulate the angular extent of the real solar disk. Light from the source enters through an aperture the class 100 clean room, where the stray light measurement set-up is installed. The detector is a photodiode (Newport 818-SL), with a baffle holding a 0.45 mm pin-hole, to allow high angular resolution. A light trap is placed very near to the detector, in order to prevent direct “solar” disk light from being scattered inside the room. Stray light measurements were performed behind the linear occulter along a direction perpendicular to the occulter edge.

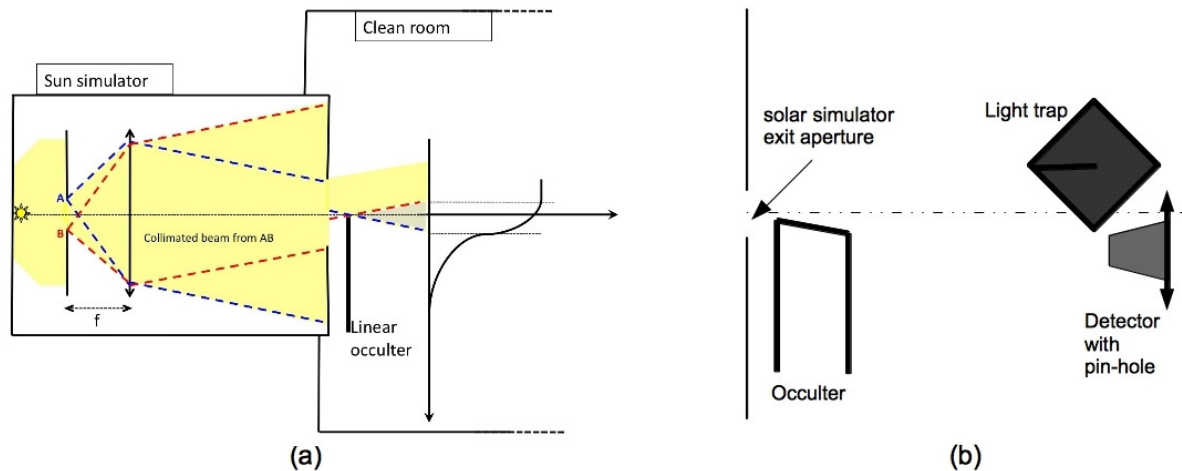


Fig. 4. Sketch of the measurement set-up. (a) Overview of the complete set-up, divided in two separated rooms, communicating only by the exit aperture of the source. (b) Detailed view of the optics set-up for stray light measurement behind the occulter

All measurements are relative to the source unobstructed flux (i.e., without occulter mounted). In order to simulate the change in the inclination of the cone surface, the linear occulter was mounted on a metal plate fixed on a precision steel tilting platform (Newport TGN-80). This also helped defining the tolerance we can allow in manufacturing the occulters, by repeating the stray light measurement at slightly different angles.

C. Conic occulter

With the set-up described in the previous subsection, various conic configurations have been applied to the linear occulter. The longitudinal dimension of the cone is only one of the issues to be investigated in our tests. In order to understand how materials, surface polishing, scratches and assembling errors affect the stray light reduction performances, we performed several indicative tests, for each of which a different occulter was designed and manufactured. There are not appreciable differences in stray light reduction performances either by changing material from Aluminum to Invar, or by scratching the Aluminum surface, if the scratches depth is kept within 20 μm . The comparison between two lengths, 10 cm and 15 cm, is shown in Fig. 5 together with the stray light measured behind a knife-edge (in red), that perfectly fits the theoretical behaviour. A further test made by repeating the measurement with the same conic occulter but with different cone angles, revealed that the tolerance in manufacturing the cone angle is about 2 arcmin (i.e., within 2 arcmin there are not appreciable deviations from the expected performances in stray light reduction).

D. Toroidal occulters

In subsection A, we stated that a barrel designed along the same principles used for multiple disks systems, cannot appreciably deviate from a cone. In any case, we can arbitrarily change the barrel designing principle, and compare its performances with the conic occulter. We designed three different linear occulters with a cylinder-like geometry that would be viewed as toroidal occulters in the case of the ASPIICS geometry.

These occulters were made of electro-eroded aluminum and differ from each other by their radius of curvature. In order to investigate the widest possible range of geometries, we chose to adopt radii of 1 cm, 10 cm, and 1 m. The corresponding results are shown in Fig. 5. Their performances in stray light reduction are better than the simple knife-edge, but not as good as the conic occulter. It is also interesting to note that by flattening the toroidal surface (i.e., by increasing its radius of curvature), the performances improve.

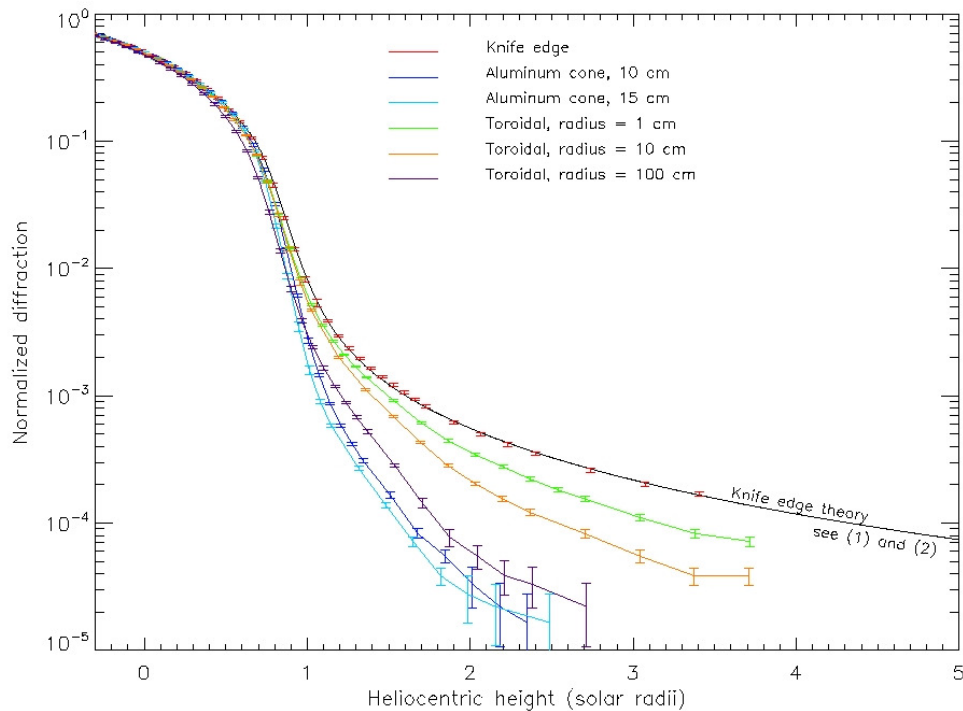


Fig. 5. Profiles of the diffracted light behind different linear occulters

V. CONCLUSION

ASPIICS is a space-borne solar coronagraph selected by ESA for the PROBA-3 formation flight mission. The coronagraph will be distributed on two spacecrafts (one with the external occulter, the other with the telescope), separated by 150 m. The present paper deals with stray light analysis, that is one of the most critical issues in designing coronagraphs. We investigated both theoretical and experimental aspects of the matter.

In order to lower the stray light on the IO plane, we designed a set of baffles to be mounted inside the telescope structure, and a tube with a series of internal vanes to be installed in front of the entrance pupil. We simulated different roughnesses for the telescope mirrors in order to measure their impact on the stray light level at the focal plane, and finally we calculated the stray light pattern at the IO plane, given by the light diffracted by the external occulter and propagated through the telescope.

Moreover, we started the investigation for the optimization of the external occulter. Since it is practically impossible to realize a full-scale model of ASPIICS, we designed a set-up able to measure the stray light behind a section of the whole occulter, using a solar simulator as source. The section of such a large occulter (1.5 m diameter) can be well approximated by a small straight edge piece. All our measurements have been relative to the source unobstructed flux and had the knife edge performance as reference. We compared together several types of occulters. The best solution in terms of stray light reduction is the model for a conic occulter, as long as possible along the optical axis.

REFERENCES

- [1] P. Lamy et al., "ASPIICS: a giant, white light and emission line coronagraph for the ESA PROBA-3 Formation Flying Mission", this conference.
- [2] J.W. Evans, "Photometer for measurement of sky brightness near the sun", *J. Opt. Soc. Am.*, vol. 38, p. 1083, 1948.
- [3] M. Born and E. Wolf, *Principles of Optics*, 7th ed., Cambridge: Cambridge University Press, pp. 476-484, 2002.
- [4] A.V. Lenskii, "Theoretical evaluation of the efficiency of external occulting systems for coronagraphs", *Sov. Astron.*, vol. 25, pp. 366-372, 1981.
- [5] S. Koutchmy, "Space-borne coronagraphy", *Sp. Sc. Rev.*, vol. 47, pp. 95-143, 1988.
- [6] M. Bout, P. Lamy, A. Maucherat, C. Colin, and A. Llebaria, "Experimental study of external occulters for the Large Angle and Spectroscopic Coronagraph 2: LASCO-C2", *App. Opt.*, vol. 39, pp. 3955-3962, 2000.